Progress In Electromagnetics Research M, Vol. 13, 261–273, 2010

A PLANAR FOCUSING ANTENNA DESIGN USING QUASI-CONFORMAL MAPPING

Z. L. Mei †, **J. Bai, and T. M. Niu**

School of Information Science and Engineering
Lanzhou University
Lanzhou 730000, China

T. J. Cui

State Key Laboratory of Millimeter Waves
Department of Radio Engineering
Southeast University
Nanjing 210096, China

Abstract—We propose a planar focusing antenna design, which has the same performance as its parabolic counterparts and can be realized using PEC-backed gradient index dielectrics. In this design, quasi-conformal transformation optics is first utilized to transform a parabolic surface into a planar one, then the anisotropy factor of the resultant material is minimized, and the material is approximately treated as isotropic. Examples with realizable material parameters are given, and the simulation results validate the design. The proposed method could be used to design planar focusing antennas with high directivity and similar devices. The idea can also be applied to new device designs in optics engineering.

1. INTRODUCTION

In 2006, Pendry and his coworkers theoretically designed an invisibility cloak [1], which was soon verified experimentally by Smith et al. in the microwave regime [2]. Their success has aroused great interests, and the method, transformation optics, coupled with the emerging metamaterial technology, has been intensively explored in various designs such as cloaks [3–13], perfect lenses [14–16],

Corresponding author: Z. L. Mei (meizl@lzu.edu.cn).
† Also with State Key Laboratory of Millimeter Waves, Department of Radio Engineering Southeast University, Nanjing 210096, China.

concentrators [17, 18], and other novel devices [19–21]. Being an indispensable part in telecommunication systems, many new types of antennas have also been proposed based on this powerful tool [22–29].

An awkward situation with transformation optics is that the resulting materials are, in most cases, inhomogeneous and anisotropic, and may have singular-valued material parameters [30, 31], which severely hinders the practical implementation. To deal with this problem, one straight-forward way is to limit the polarization of the incident wave and reduce the number of material parameters in Maxwell's equations. Simplified material parameters are also proposed based on the dispersion equation in anisotropic materials [2, 4]. Another important method based on functional theory is to optimize the transformation function so that only inhomogeneous and isotropic parameters can be achieved [5]. Under this circumstance, the resulting transformation function is called quasi-conformal mapping, which is more general than classical conformal mapping. As an example, carpet cloaks working at the microwave and optical frequencies have been successfully verified by experiments [6–8, 13]. Very recently, quasi-conformal mapping transformation optics has also been utilized to flatten the traditional Luneburg lens, and satisfactory results are reported [32].

In this work, we make use of the transformation optics based on quasi-conformal mapping to design a directive and planar focusing antenna, which has similar performance as a parabolic dish and can be realized using PEC-backed gradient-index materials. These gradient-index materials can be easily implemented with either non-resonant metamaterials or nonmagnetic dielectrics based on the effective medium theory [6, 33]. Thus the antenna is broadband in nature and could be scaled down to optical frequencies. We believe that the proposed method and designed antenna have wide applications in the communication sectors and the design of solar cells.

2. THEORETICAL ANALYSIS

Figure 1 shows the virtual (a) and physical (b) spaces concerned with the antenna design, which is the basis for the transformation optics method. In the virtual space, the curved boundary represents a two-dimensional (2D) parabolic dish, which can be expressed as $6y = (x-2)^2 - 1$. The aperture of the dish is 2 meters, and the focal distance is 1.5 m. The antenna is fed by a 2D point source at the focal point. It is obvious that the radiated fields will be reflected by the dish and generally propagate along the vertical direction, and the device can have a high directivity. The region bounded by

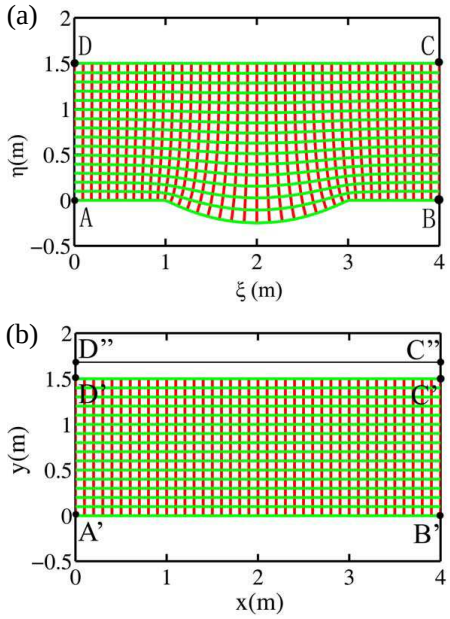

Figure 1. Quasi-conformal mapping between the (a) virtual and (b) physical spaces. The green (horizontal) and red (vertical) lines show the corresponding mapping between such two spaces.

the rectangle and parabolic curve, including the point source, is the solution domain in the virtual space. Using a deliberately designed coordinate transformation, the solution domain is transformed into a rectangular region in the physical space. Note that only the bottom boundary is compressed to flatten the curved segment (slipping boundary condition), and other boundaries are unchanged. From the theory of transformation optics, we know that the resultant device, a PEC-backed metamaterial with the rectangular shape, will have the same electrical performance as the original parabolic dish (outside the rectangular region).

Generally speaking, the resulting materials in the rectangular region of the physical space are inhomogeneous and anisotropic, and the electric permittivity tensor is given by

$$\overline{\overline{\varepsilon}}' = A\overline{\overline{\varepsilon}}A^{\mathrm{T}}/\det(A) \tag{1}$$

in which A is the Jacobian matrix between the two spaces [30, 31]. The same formula holds for the magnetic permeability tensor. Similar results have been obtained by Kong et al. in the planar antenna

design [26]. We note that for the given virtual and physical spaces, there exist infinite number of transformations that can realize the corresponding mapping, among which some can be expressed analytically, while others can only be calculated numerically [1, 19]. However, if we optimize the transformation function between the two spaces, we can then minimize the anisotropy of the metamaterial and treat it as an isotropic one. As a consequence, the metamaterial is easily realizable. This is the major difference between the present work and that in [26].

Suppose that we are analyzing the TE mode (Electric field normal to the transformation plane. TM results can be obtained using the principle of duality), then the material parameters in Eq. (1) can be further written as

$$\varepsilon' = 1/\det(A), \quad \overline{\overline{\mu}}' = AA^{\mathtt{T}}/\det(A) \tag{2}$$

where A, in this 2D situation, is given by

$$A = \begin{pmatrix} \frac{\partial x}{\partial \xi} & \frac{\partial x}{\partial \eta} \\ \frac{\partial y}{\partial \xi} & \frac{\partial y}{\partial \eta} \end{pmatrix}. \tag{3}$$

Note that the virtual space is supposed to be a vacuum with $\varepsilon = \mu = 1$. From Eqs. (2), it is easy to see that the anisotropy goes to the permeability tensor. Since this is a symmetric quantity, it can be easily diagonalized in the principal system, i.e., $\overline{\overline{\mu}}' = \Lambda(\mu_T, \mu_L)$, with $\mu_T \mu_L = 1$. And the following anisotropy factor for the permeability tensor can be defined [5], which is

$$\alpha = \max(\sqrt{\mu_T/\mu_L}, \sqrt{\mu_L/\mu_T}). \tag{4}$$

Using the basic knowledge of linear algebra, it is not difficult to get the following formula

$$\alpha + 1/\alpha = \mathrm{Tr}(g)/\sqrt{\det(g)}, \tag{5}$$

where g is the metric tensor and $g = A^T A$.

If α can be minimized in the entire solution domain, then the anisotropy can be minimized at the same time. And this is achieved by minimizing the Modified-Liao functional [34]

$$\Phi = \int\int \frac{\mathtt{Tr}(g)^2}{\det(g)} d\xi d\eta. \tag{6}$$

Without going further into the technical detail, we borrow the results given by [5] that the minimal for this functional occurs at the quasi-conformal map, which can be numerically calculated using grid generation techniques or through solving the Laplace's

equation [19, 34, 35]. In this paper, the mapping is obtained through the following two steps [36]. First, the quasi-rectangle domain $ABCD$ in the virtual space is conformally transformed into a rectangle, which is represented as $A'B'C''D''$ in Fig. 1(b). The points A, B, C and D in the virtual space are mapped respectively to A', B', C'' and D'' in the counter-clockwise order. According to complex analysis, this rectangle must have a specific aspect ratio, $M = |A'B'|/|A'D''|$, which is defined as the conformal modulus for generalized quadrilaterals. In our work, it can be calculated using $M = |A'B'|/\int_{AD} |\frac{\partial x}{\partial n}|dl$. Then, as the second step, the rectangle $A'B'C''D''$ is scaled to $A'B'C'D'$ in the physical space, which is shown in Fig. 1(b) too. As given by Zhang et al. [36], strict conformal mappings do not produce any anisotropy, and the anisotropy only occurs during the second step since the two rectangles may have different aspect ratios, or conformal modului. As a result, the anisotropy factor can be further expressed as $\alpha = \max(M/m, m/M)$ [5, 36], where m is the aspect ratio for the physical space, and $m = |A'B'|/|A'D'|$. If this value is very close to 1, then magnetic parameters can be approximately treated as isotropic (Identity tensor in this case), and the following refractive index can be defined

$$n^2 = \varepsilon' = 1/\det(A). \tag{7}$$

Please note that the above two situations concerning Eqs. (2) and (7) are referred to as anisotropic and isotropic cases respectively in the following discussion.

In Fig. 1, we also show the proposed quasi-conformal mapping between the two spaces with colored grids. Note that all grids are orthogonal ones due to quasi-conformal mapping. It should also be noted that for the proposed coordinate transformation with quasi-conformal mapping, the deformation between the physical and virtual spaces cannot be large so that the anisotropy ratio is nearly 1 [5, 32, 36]. This explains why we should include a bulky rectangular area in the solution domain in the virtual space.

Figure 2 gives the refractive index distribution inside the planar antenna. It can be seen in Fig. 2(a) that the refractive index varies from 0.44 to 1.29. The variation is larger in the vicinity of the PEC plane, with larger values in the center and smaller values around the two ends. It is easily understood since this part is transformed from the curved region in the virtual space and corresponds to the severest deformation in the mapping. For most part of the device, the refractive index gradually changes with position and is roughly equal to 1. Though metamaterials can be utilized to realize the permittivity less than 1, they may involve resonant structures and limit the working bandwidth. To further reduce the difficulties encountered, we can set

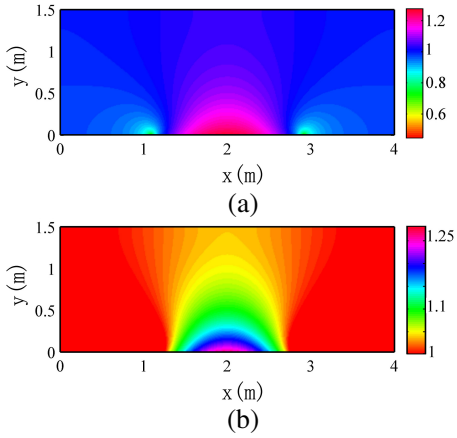

Figure 2. The profile of the refractive index for the proposed planar focusing antenna. (a) The isotropic case with some parameters less than 1; (b) The modified case with all the parameters larger than 1.

all the refractive indices below 1 to 1. This modification, of course, leads to some performance degradation, but we will show that it is not severe. The modified profile is given in Fig. 2(b), and the antenna using such a profile is considered as the modified case in the following part.

As mentioned earlier, the device is a little bulky for practical usage. This problem can be partly solved by carefully 'cutting' the device into a slim one. A careful examination in Fig. 2(b) reveals that the high refractive-index values are mainly concentrated in a small region near the PEC plane, while the values approaching 1 occupy most part of the device. Hence it is possible to reduce the size without severe performance deterioration. The cut antenna is referred to as the slim case hereafter.

3. SIMULATION RESULTS AND DISCUSSION

The correctness of the proposed method and the designed antenna are demonstrated by the following numerical calculations. In our simulations, the finite-element based commercial software, COMSOL MULTIPHYSICS, is used along with homemade Matlab codes. In all simulations, the transverse-electric (TE) mode is utilized. For the sake of clarity, we treat the above mentioned cases as anisotropic, isotropic, modified and slim cases, respectively.

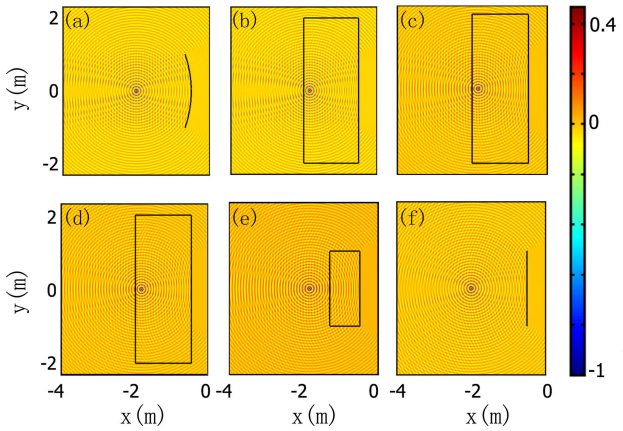

Figure 3. The normalized electric-field distributions in the nearfield region. (a) A parabolic dish. (b) The planar antenna with anisotropic materials. (c) The planar antenna with isotropic materials. (d) The planar antenna with modified parameters having the loss tangent of 0.001. (e) The slim version of (d). (f) A PEC plate. In our simulations, the area of the rectangular region is about $4\,\mathrm{m} * 1.5\,\mathrm{m}$, the planar antenna lies at $x = -0.5\,\mathrm{m}$, and the working frequency is 4 GHz. The slim antenna is $2\,\mathrm{m} * 0.8\,\mathrm{m}$ in size, about one quarter of the original size.

Figure 3 shows the distribution of the electric fields in the near-field region under different situations. Fig. 3(a) gives the distribution for a parabolic dish, and Fig. 3(b) shows the electric field distribution for the proposed planar antenna with anisotropic material parameters. It can be seen that these two distributions are exactly the same, a direct consequence of the invariance of Maxwell's equation under the coordinate transformation. In Fig. 3(c), we show the isotropic case, with the presence of material parameters less than 1. It is found that some disparities occur between (a)/(b) and (c). However, the field distribution of the device looks similar to that of the parabolic dish (or the anisotropic case), and the directive radiation is clearly observed. For practical reasons, we then consider the modified case with all material parameters larger than 1. The simulation result is demonstrated in Fig. 3(d). Note that losses are also added in the modified case with the loss tangent of 0.001. Not-surprisingly, the modified and lossy material parameters, which can be easily realized and have practical significance, produce similar results, and the difference between Figs. 3(c) and (d) is small. The simulation

results for the slim antenna are illustrated in Fig. 3(e) with the same loss. Under this situation, the field distribution changes a little, and the main beam becomes wider than the former cases. However, the general pattern is preserved which clearly shows the correctness of the size reduction proposal. Another gain from the size reduction is that the point source can now be implemented outside the material region, which gives more flexibility and is a necessity for some situations. We remark that the performances of the device is not simply due to the presence of the PEC plate, a case shown in Fig. 3(f). It is seen that the field distribution is totally different from the previous cases. This is a strong support for the deliberately designed gradient-index materials.

To quantitatively verify the above designs, we calculate the far-field radiation patterns for the parabolic dish and the proposed planar antennas. The calculation is based on the near-far field transformation technique. At first, the near field data are collected along a circle surrounding the antenna, then Huygens' principle is used to get the far field information. The same method has been utilized by other researchers and proved to be effective in various situations [13, 25, 29, 37]. Fig. 4 gives the corresponding results for the above designs. In Fig. 4, we notice that the far-field pattern for the anisotropic case (the red curve) is nearly the same as that of the parabolic dish (the blue line). For the isotropic (the cyan line) and modified and lossy cases (the magenta line), the radiation patterns are similar to that of the parabolic dish. Larger differences are found near the side lobes, and the width of the main lobe is slightly widened. However, the side lobe levels are lowered at the same time, a very good property for the directive radiation. This fact firmly supports our designs using practical dielectric materials. In Fig. 4, the black curve, which looks totally different from other curves, represents the far field pattern for a bare PEC plate. This fact strongly indicates the necessity of the designed materials.

The main-lobe widening phenomenon is mainly due to the approximate treatment of the anisotropic parameters as isotropic ones. In our simulations, the anisotropy ratio after quasi-conformal mapping is about 1.0318. To treat it as 1 is acceptable but leads to the performance degradation [36], i.e., the main-lobe expansion in the far field. However, the resulting antenna still has high directivity. In Fig. 4, the half power beam width is less than 5 degrees for the modified and lossy antenna. Even for the slim and lossy case (the green curve), in which the main lobe is the widest, the half power width is still less than 10 degrees. This is a very fascinating property for the proposed design.

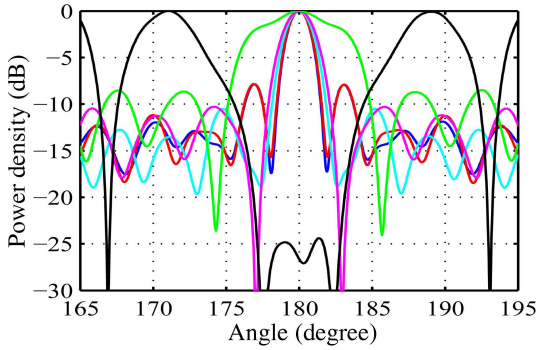

Figure 4. The normalized power density in the far-field region for the cases listed in Fig. 3. The blue, red, cyan, magenta, green and black curves (from the inner side of the peak to the outer side) correspond to cases (a)–(f), respectively, in Fig. 3. Note that the curve for case (f) is totally different from other curves.

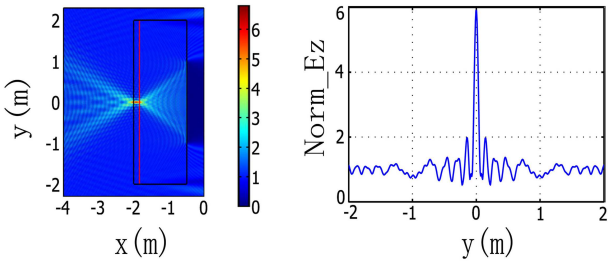

Figure 5. (a) The magnitude (norm of the field) distribution of the electric field when a plane wave impinges on the proposed antenna along the x direction at 4 GHz. (b) The cross-section plot along the red line in (a). The calculated focal point is located at $(-1.8423; 0)$.

Up to now, we have numerically verified that a point source embedded in the PEC-backed dielectric material has a high directive radiation. Based on the reciprocity theorem, a plane wave illuminating on the antenna can also produce a focal point inside the device. Fig. 5 shows the corresponding magnitude distribution. It is seen that when a plane wave strikes the antenna along the x-axis direction, the wave will be reflected to form a focus. The cross-section plot on the focal plane further proves our designs. This property, together with its planar structure, will have potential applications in solar cell designs.

We remark that the proposed method and the designed structure can also be scaled down to the optical field since no magnetic materials

are needed. Actually, similar 'scale down' has been proved for the carpet cloaks, which are also based on the quasi-conformal mapping method and implemented using gradient index dielectrics, and some also involve a PEC plate in the configuration. Such cloaks have already been realized and verified in the microwave and optical regime very recently [6–8].

We emphasize that the basis for our planar antenna design lies in the fact that the resultant anisotropy ratio approaches 1 after quasi-conformal mapping. We also note that an arbitrary parabolic curve and an arbitrarily-sized rectangle are used in the simulation, and only a few efforts are spent on the optimization of its geometry. If an optimized structure is selected with the above conditions met, it is certain that the corresponding planar antenna will give even better performances. In this regard, parabolas with the same aperture but longer focal length are preferred. However, one has to make a compromise among its electrical performance, the geometrical size and the realizability of the final system. Moreover, the planar structure in the physical domain can be modified to other shapes (e.g., another quasi-rectangle with a curved boundary for the bottom line), and they can still be designed to have similar performance to the parabolic reflector. This will have potential applications in the conformal antenna designs. Moreover, we use the isotropic feed in the design, which can be further improved by using less directive radiation elements, such as horn antennas, dipole antennas etc.

4. CONCLUSION

In conclusion, we have proposed a novel planar focusing antenna design, which has high directivity as its parabolic counterpart and can be realized using the gradient-index materials. In fact, the antenna can be implemented by using either the ordinary dielectrics (e.g., through drilling sub-wavelength hole arrays [33]) or the non-resonant metamaterials (e.g., I-shaped unit cells [6]), which has broad bandwidth, low loss and is easily realizable. Moreover, the device can be scaled down to work at the optical frequencies. The proposed device can find applications in the design of antennas and for the efficient solar energy harvest.

ACKNOWLEDGMENT

This work was supported in part by a Major Project of the National Science Foundation of China under Grant Nos. 60990320 and 60990324, in part by the Natural Science Foundation of Jiangsu Province under Grant No. BK2008031, in part by the 111 Project

under Grant No. 111-2-05, and in part by the National Science Foundation of China under Grant Nos. 60871016, 60901011, and 60921063. Z. L. Mei acknowledges the support from the China Postdoctoral Science Foundation (No. 20080441006), the Fundamental Research Funds for the Central Universities (No. LZUJBKY-2009-61), the Inter-Discipline Science Foundation of Lanzhou University (No. LZUJC2007001), and the Natural Science Foundation of Gansu Province (No. 0803RJZA029).

REFERENCES

1. Pendry, J. B., D. Schurig, and D. R. Smith, "Controlling electromagnetic fields," *Science*, Vol. 312, 1780–1782, 2006.
2. Schurig, D., J. J. Mock, B. J. Justice, S. A. Cummer, J. B. Pendry, A. F. Starr, and D. R. Smith, "Metamaterial electromagnetic cloak at microwave frequencies," *Science*, Vol. 314, 977–980, 2006.
3. Leonhardt, U., "Optical conformal mapping," *Science*, Vol. 312, 1777–1780, 2006.
4. Cai, W., U. K. Chettiar, A. V. Kildishev, and V. M. Shalaev, "Optical cloaking with metamaterials," *Nat. Photon.*, Vol. 1, 224–227, 2007.
5. Li, J. and J. B. Pendry, "Hiding under the carpet: A new strategy for cloaking," *Phys. Rev. Lett.*, Vol. 101, 203901, 2008.
6. Liu, R., C. Ji, J. J. Mock, J. Y. Chin, T. J. Cui, and D. R. Smith, "Broadband ground-plane cloak," *Science*, Vol. 323, 366–369, 2009.
7. Valentine, J., J. Li, T. Zentgraf, G. Bartal, and X. Zhang, "An optical cloak made of dielectrics," *Nat. Materials*, Vol. 8, 568–571, 2009.
8. Gabrielli, L. H., J. Cardenas, C. B. Poitras, and M. Lipson, "Silicon nanostructure cloak operating at optical frequencies," *Nat. Phonotics*, Vol. 3, 461–463, 2009.
9. Smolyaninov, I. I., V. N. Smolyaninova, A. V. Kildishev, and V. M. Shalaev, "Anisotropic metamaterials emulated by tapered waveguides: Application to optical cloaking," *Phys. Rev. Lett.*, Vol. 102, 213901, 2009.
10. Cheng, Q., W. X. Jiang, and T. J. Cui, "Investigations of the electromagnetic properties of three-dimensional arbitrarily-shaped cloaks," *Progress In Electromagnetics Research*, Vol. 94, 105–117, 2009.
11. Lai, Y., H. Chen, Z. Q. Zhang, and C. T. Chan, "Complementary

media invisibility cloak that cloaks objects at a distance outside the cloaking shell," *Phys. Rev. Lett.*, Vol. 102, 093901, 2009.

12. Lai, Y., J. Ng, H. Y. Chen, D. Z. Han, J. J. Xiao, Z. Q. Zhang, and C. T. Chan, "Illusion optics: The optical transformation of an object into another object," *Phys. Rev. Lett.*, Vol. 102, 253902, 2009.
13. Ma, H. F., W. X. Jiang, X. M. Yang, X. Y. Zhou, and T. J. Cui, "Compact-sized and broadband carpet cloak and free-space cloak," *Opt. Express*, Vol. 17, 19947–19959, 2009.
14. Wang, W., L. Lin, X. Yang, J. Cui, C. Du, and X. Luo, "Design of oblate cylindrical perfect lens using coordinate transformation," *Opt. Express*, Vol. 16, 8094–8105, 2008.
15. Tsang, M. and D. Psaltis, "Magnifying perfect lens and superlens design by coordinate transformation," *Phys. Rev. B*, Vol. 77, 035122, 2008.
16. Kwon, D. and D. H. Werner, "Transformation optical designs for wave collimators, flat lenses and right-angle bends," *New J. Phys.*, Vol. 10, 115023, 2008.
17. Rahm, M., D. Schurig, D. A. Roberts, S. A. Cummer, D. R. Smith, and J. B. Pendry, "Design of electromagnetic cloaks and concentrators using form-invariant coordinate transformations of Maxwell's equations," *Photonics Nanostruct. Fund. Appl.*, Vol. 6, 87–95, 2008.
18. Jiang, W. X., T. J. Cui, Q. Cheng, J. Y. Chin, X. M. Yang, R. Liu, and D. R. Smith, "Design of arbitrarily shaped concentrators based on conformally optical transformation of nonuniform rational B-spline surfaces," *Appl. Phys. Lett.*, Vol. 92, 264101, 2008.
19. Chang, Z., X. Zhou, J. Hu, and G. Hu, "Design method for quasi-isotropic transformation materials based on inverse Laplace's equation with sliding boundaries," *Opt. Express*, Vol. 18, 6089–6096, 2010.
20. Ma, Y. G., N. Wang, and C. K. Ong, "Application of inverse, strict conformal transformation to design waveguide devices," *J. Opt. Soc. Am. A*, Vol. 27, 968–972, 2010.
21. Landy, N. I. and W. J. Padilla, "Guiding light with conformal transformations," *Opt. Express*, Vol. 17, 14872–14879, 2009.
22. Enoch, S., G. Tayeb, P. Sabouroux, N. Guérin, and P. Vincent, "A metamaterial for directive emission," *Phys. Rev. Lett.*, Vol. 89, 213902, 2002.
23. Zhang, J., Y. Luo, H. Chen, and B. Wu, "Manipulating the

directivity of antennas with metamaterial," *Opt. Express*, Vol. 16, 10962–10967, 2008.

24. Duan, Z. Y., B.-I. Wu, J. A. Kong, F. M. Kong, and S. Xi, "Enhancement of radiation properties of a compact planar antenna using transformation media as substrates," *Progress In Electromagnetics Research*, Vol. 83, 375–384, 2008.
25. Jiang, W. X., T. J. Cui, H. F. Ma, X. M. Yang, and Q. Cheng, "Layered high-gain lens antennas via discrete optical transformation," *Appl. Phys. Lett.*, Vol. 93, 221906, 2008.
26. Kong, F., B.-I. Wu, J. A. Kong, J. Huangfu, S. Xi, and H. Chen, "Planar focusing antenna design by using coordinate transformation technology," *Appl. Phys. Lett.*, Vol. 91, 253509, 2007.
27. Tichit, P. -H., S. N. Burokur, and A. de Lustrac, "Ultradirective antenna via transformation optics," *J. Appl. Phys.*, Vol. 105, 104912, 2009.
28. Ma, Y. G., P. Wang, X. Chen, and C. K. Ong, "Near-field plane-wave-like beam emitting antenna fabricated by anisotropic metamaterial," *Appl. Phys. Lett.*, Vol. 94, 044107, 2009.
29. Ma, H. F., X. Chen, H. S. Xu, X. M. Yang, W. X. Jiang, and T. J. Cui, "Experiments on high-performance beam-scanning antennas made of gradient-index metamaterials," *Appl. Phys. Lett.*, Vol. 95, 094107, 2009.
30. Leonhardt, U. and T. G. Philbin, "General relativity in electrical engineering," *New J. Phys.*, Vol. 8, 247, 2006.
31. Milton, G. W., M. Briane, and J. R. Willis, "On cloaking for elasticity and physical equations with a transformation invariant form," *New J. Phys.*, Vol. 8, 248, 2006.
32. Kundtz, N. and D. R. Smith, "Extreme-angle broadband metamaterial lens," *Nat. Material*, Vol. 9, 129–132, 2009.
33. Mei, Z. L., J. Bai, and T. J. Cui, "Gradient index metamaterials realized by drilling hole arrays," *J. Phys. D: Appl. Phys.*, Vol. 43, 055404, 2010.
34. Knupp, P. and S. Steinberg, *Fundamentals of Grid Generation*, CRC Press, Boca Raton, 1994.
35. Thompson, J. F., B. K. Soni, and N. P. Weatherill, *Handbook of Grid Generation*, CRC Press, Boca Raton, 1999.
36. Zhang, B., T. Chan, and B.-I. Wu, "Lateral shift makes ground-plane cloak detectable," *Phys. Rev. Lett.*, Vol. 104, 233903, 2010.
37. Li, C. and F. Li, "Two-dimensional electromagnetic cloaks with arbitrary geometries," *Opt. Express*, Vol. 16, 13414–13420, 2008.